

Supporting Information

For

Ion mobility mass spectrometry – efficient tool for analysis of conformational switch of macrocyclic receptors upon anion binding

Magdalena Zimnicka,^{*a} Elina Kalenius,^b Janusz Jurczak,^a and Witold Danikiewicz^a

^a Institute of Organic Chemistry, Polish Academy of Sciences, Kasprzaka 44/52, 01-224 Warsaw, Poland

^b Department of Chemistry, Nanoscience Center, University of Jyväskylä, FI-40014 Jyväskylä, Finland

^{*}Corresponding author: magdalena.zimnicka@icho.edu.pl

Table of Contents

Section S1. DTIM-MS Measurements.....	S3
S1.1. General Information	S3
Table S1.1. Summary of the DTIM-MS measurements.	S3
Figure S1.1. (-)ESI-QTOF mass spectra and drift-time arrival time distributions.....	S4
Section S2. Traveling-wave ion mobility spectrometry measurements	S6
S2.1. General information	S6
Table S2.1. Supporting data to Figure 4	S6
Figure S2.1. Relationship between ${}^{\text{DT}}\text{CCS}_{\text{N}_2}$ and ${}^{\text{TW(PA)}}\text{CCS}_{\text{N}_2}$ values	S7
Figure S2.2. Relationship between the calibration plots (He) for deprotonated polyalanine ions (Ala_n , $n = 4 - 10$) and macrocyclic ions: $[\text{M} - \text{H}]^-$ and $[\text{M} + \text{Cl}]^-$	S7
Table S2.2. ${}^{\text{TW(PA)}}\text{CCS}_{\text{N}_2}$ and ${}^{\text{TW(PA)}}\text{CCS}_{\text{He(N}_2)}$ values of $[\text{M} - \text{H}]^-$ and $[\text{M} + \text{Cl}]^-$	S8
Table S2.3. TWIM-experimental values and calibration parameters	S9
Table S2.4. CCS determination of $[\mathbf{1} + \text{X}]^-$ complexes. TWIM-experimental data.....	S14
Figure S2.3. CCS determination of $\mathbf{1} + \text{X}^-$ complexes. Calibration plots	S16
Table S2.5. ${}^{\text{TW(M)}}\text{CCS}$ and ${}^{\text{TW(PA)}}\text{CCS}$ values of $[\mathbf{1} + \text{X}]^-$ complexes	S17
Table S2.6. CCS determination of $[\mathbf{5} + \text{X}]^-$ complexes. TWIM-experimental data.....	S18
Table S2.7. ${}^{\text{TW(M)}}\text{CCS}$ and ${}^{\text{TW(PA)}}\text{CCS}$ values of $[\mathbf{5} + \text{X}]^-$ complexes	S20
Section S3. Theoretical Computations	S21
S3.1. General Information	S21
S3.2. CCS values prediction.....	S21
Table S3.1 Differences between theoretically predicted and experimental CCS values of $[\text{M} - \text{H}]^-$ and $[\text{M} + \text{Cl}]^-$	S22
Figure S3.1. Structures of the lowest-energy conformers of deprotonated and chloride adducts of macrocycles 1-5 (view on a mean plane of macrocyclic ring).....	S23
Figure S3.2. Differences in bond lengths and partial charges on Cl^- of the most stable structures $[\mathbf{1} + \text{Cl}]^-$ calculated with B3LYP and PBE0 methods.....	S24
Table S3.2. Theoretically predicted ${}^{\text{TM}}\text{CCS}$ values of $[\mathbf{1} + \text{X}]^-$	S25
Table S3.3. Theoretically predicted ${}^{\text{TM}}\text{CCS}$ values in N_2 and He of polyatomic anions	S26
Figure S3.3. Overlapped structures of selected $[\mathbf{1} + \text{X}]^-$ complexes.....	S26
Table S3.4. Theoretically predicted ${}^{\text{TM}}\text{CCS}$ values of $[\mathbf{5} + \text{X}]^-$	S27
References.....	S28

Section S1. DTIM-MS Measurements

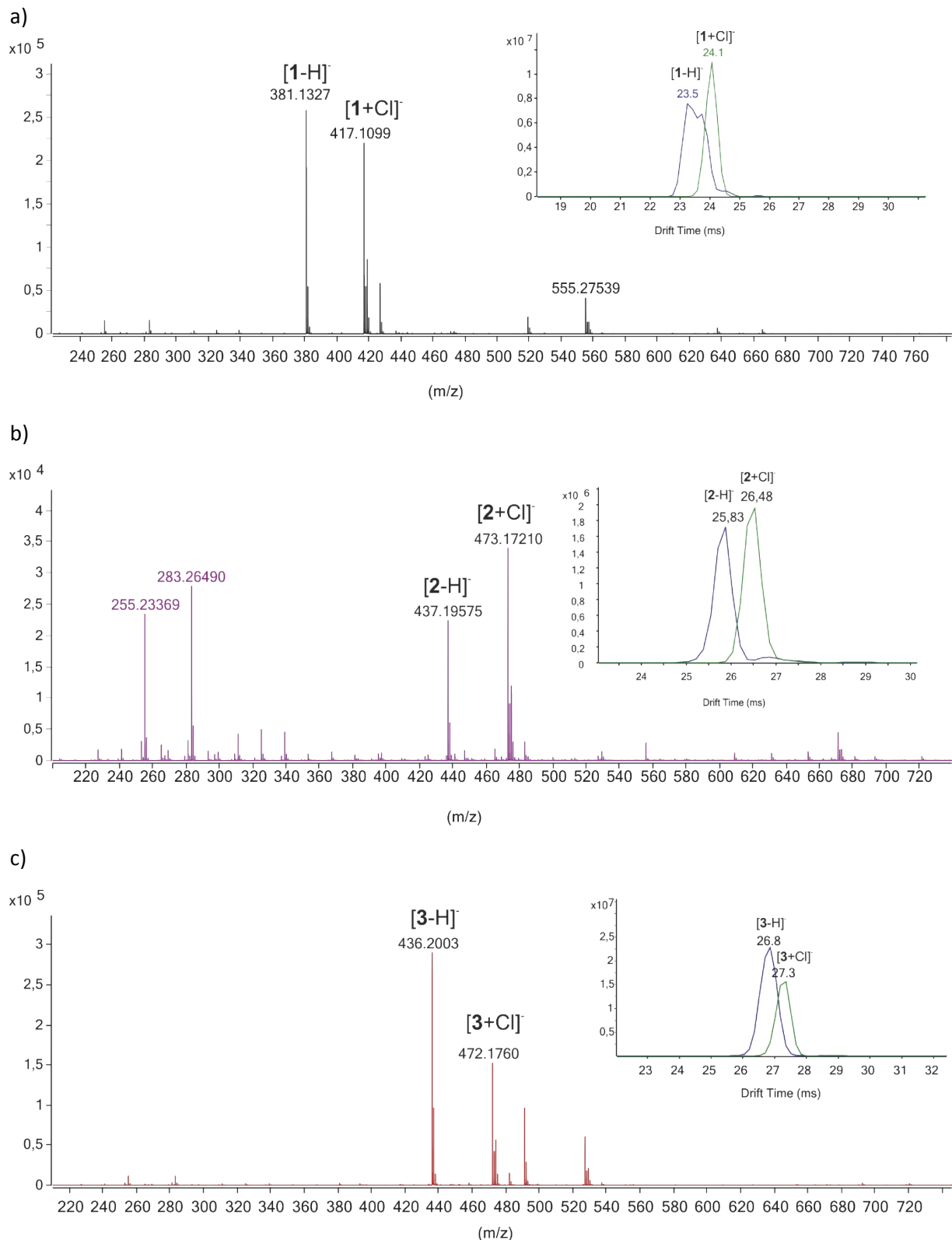
S1.1. General Information

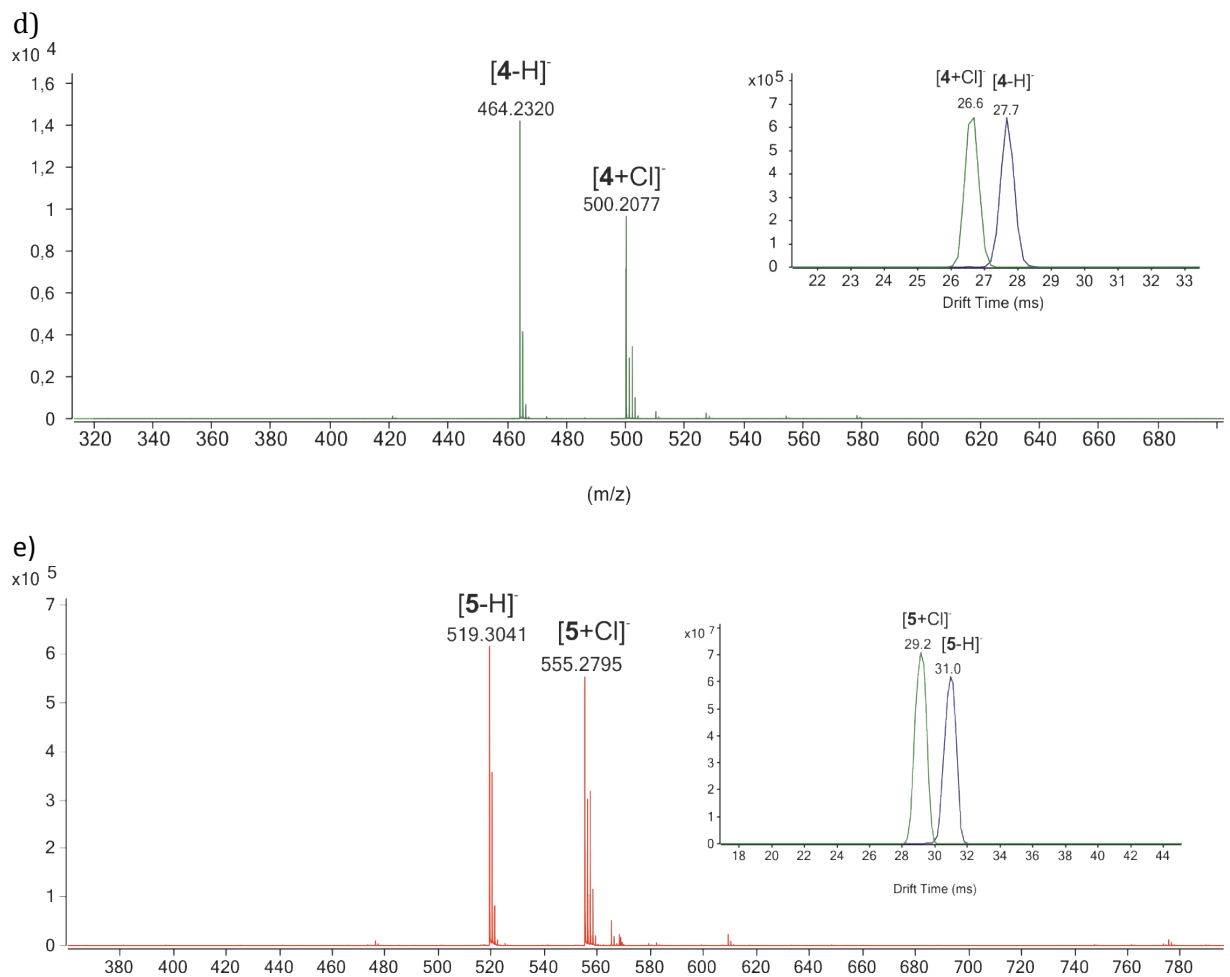
Direct, drift tube ion mobility mass spectrometry (DTIM-MS) experiments were performed on Agilent 6560 Ion mobility Q-TOF mass spectrometer, which was equipped with a dualESI ion source. Samples were injected from a syringe pump with a 5 $\mu\text{l}/\text{min}$ flow rate. Nitrogen was used as a drying gas with a temperature of 498 K, gas flow 5 l/min, and nebulizer pressure of 6 psi. Capillary voltage of 5 kV and a fragmentor voltage of 400V were set as source parameters. The drift gas pressure was 3.95 Torr and temperature 300 K. Pressure in the trap funnel was 3.80 Torr for N₂ and 3.72 Torr for He. In single-field experiments with N₂, the drift tube entrance and exit voltages were set as 1700V and 224V, respectively (for He, 800V and 133 V). As a trap, filling time 5000 μs and trap release time 350 μs were used. Before the introduction of the samples, ES tuning mix (Agilent Technologies) was measured and CCS values for its ions were determined in a multifield experiment to ensure stable conditions for CCS determination.¹⁻³ CCS values within $\pm 2 \text{ \AA}^2$ from the literature values were used as a limit to verify conditions. For multifield measurements, the drift tube entrance voltage was varied from 1074 V to 1674 V with 100 V increment for N₂ and from 563 V to 876 V with 52 V increment for He. Data was analyzed using MassHunter IM-MS Browser (Version B08.00, Agilent Technologies, USA).

Table S1.1. Summary of the DTIM-MS measurements (CCS values, reduced mobilities – K_0 , standard deviations of the determined values – SD in both N₂ and He drift gases) of macrocycles and their complexes with Cl⁻.

Ion	Formula	m/z (exp)	m/z (theor)	mass accuracy [mDa]	${}^{\text{DT}}\text{CCS}_{\text{N}_2}$ [\AA^2]	SD _{N₂} [\AA^2]	K_0 [cm ² /Vs]	${}^{\text{DT}}\text{CCS}_{\text{He}}$ [\AA^2]	SD _{He} [\AA^2]	K_0 [cm ² /Vs]
[1 - H] ⁻	C ₁₈ H ₁₇ N ₆ O ₄	381.1327	381.1317	-1	190.5	0.14	1.097	116.7	0.26	4.6
[1 + Cl] ⁻	C ₁₈ H ₁₈ N ₆ O ₄ Cl	417.1099	417.1084	-1.5	194.3	0.2	1.073	122.3	0.15	4.388
[2 - H] ⁻	C ₁₈ H ₂₅ N ₆ O ₄	437.1958	437.1943	-1.5	207.7	0.27	1.004	133.9	0.34	4.012
[2 + Cl] ⁻	C ₁₈ H ₂₆ N ₆ O ₄ Cl	473.1721	473.171	-1.1	212.5	0.27	0.979	139.2	0.17	3.857
[3 - H] ⁻	C ₂₃ H ₂₆ N ₅ O ₄	436.2003	436.199	-1.3	215.9	0.25	0.967	140.1	0.16	3.834
[3 + Cl] ⁻	C ₂₃ H ₂₇ N ₅ O ₄ Cl	472.176	472.1757	-0.3	218.8	0.26	0.952	143.2	0.15	3.748
[4 - H] ⁻	C ₂₅ H ₃₀ N ₅ O ₄	464.232	464.2303	-1.7	222.4	0.29	0.936	146.8	0.17	3.657
[4 + Cl] ⁻	C ₂₅ H ₃₁ N ₅ O ₄ Cl	500.2077	500.207	-0.7	213.2	0.24	0.974	138.9	0.16	3.866
[5 - H] ⁻	C ₃₀ H ₃₉ N ₄ O ₄	519.3041	519.2977	-6.4	248.6	0.29	0.835	167.2	0.19	3.21
[5 + Cl] ⁻	C ₃₀ H ₄₀ N ₄ O ₄ Cl	555.2795	555.2744	-5.1	231.9	0.29	0.893	156	0.21	3.441

Figure S1.1. (-)ESI-QTOF mass spectra and drift-time arrival time distributions (in insets) for macrocycles a) **1**, b) **2**, c) **3**, d) **4** and e) **5** recorded using N₂ drift gas.





Section S2. Traveling-wave ion mobility spectrometry measurements

S2.1. General information

Indirect travelling-wave ion mobility mass spectrometry (TWIM-MS) measurements were performed on a Synapt G2-S HDMS (Waters) quadrupole traveling-wave ion mobility time-of-flight mass spectrometer equipped with a standard ESI source. The mixtures of macrocycles and anion(s) were infused through a standard ESI source into the instrument at a flow rate of 10 $\mu\text{l}/\text{min}$. All measurements were performed in the negative ion mode and in the normal resolution QToF mode at m/z range of 50-1000 Da. The source parameters, being the same across various sets of traveling wave velocities and wave amplitudes, were: capillary voltage, -3.0 kV; sampling cone, 22 V; source offset, 22 V, source temperature, 353 K; desolvation temperature, 393 K; desolvation gas flow, 234 L/hr; nebulizer gas flow, 2.5 bar; ion mobility cell pressure, 4.13 mbar. Three to five sets of parameters, containing variable values of traveling wave velocity (WV) and pulse height (WH), were applied to determine the standard deviation values for the T-wave determined CCS values. The following ratios of traveling wave velocity [m/s] to wave height [V] were used: 350/29, 400/29, 450/27, 650/39, 550/29. Additionally, for each drift tube conditions, the experiments were performed in triplicate. The uncertainties of the measured CCS values associated with different drift tube conditions were estimated based on the t-test at a 95% level of confidence.

The CCS values using TWIM-MS (${}^{\text{TW}}\text{CCS}$) were obtained from calibration approach⁸. The linear or power relationship (depending on the buffer gas and ratios of traveling wave velocity to wave height; the better fit was always applied to determine CCS values) between corrected drift times and corrected collision cross sections of calibrant ions was used to determine the experimental CCS values.

Table S2.1. Supporting data to Figure 4 of the calibration plots of two sets of calibration ions: polyalanine ions ($\text{Ala}_n - \text{H}]^-$ and macrocyclic ions $[\text{M} - \text{H}]^-$ and $[\text{M} + \text{Cl}]^-$ recorded using TWIM-MS with N_2 as a drift gas. ${}^{\text{DT}}\text{CCS}_{\text{N}_2/\text{He}}$ values correspond to the reference CCS values measured by primary method for polyalanine ions and macrocyclic ions.

Ion	m/z	Arrival Time (AT)	t_d'' [ms]	${}^{\text{DT}}\text{CCS}_{\text{N}_2}$ [\AA^2]	Corrected CCS_{N_2}	${}^{\text{DT}}\text{CCS}_{\text{He}}$ [\AA^2]	Corrected CCS_{He}
$[\text{Ala}_4 - \text{H}]^-$	301.13	28.09	0.68	165.5	837.8	104	207
$[\text{Ala}_5 - \text{H}]^-$	372.16	35.15	1.06	180.6	921.8	117	233
$[\text{Ala}_6 - \text{H}]^-$	443.20	42.26	1.44	196.2	1 007.1	131	261
$[\text{Ala}_7 - \text{H}]^-$	514.23	49.13	1.80	210.3	1 083.9	143	285
$[\text{Ala}_8 - \text{H}]^-$	585.27	55.29	2.13	223.7	1 156.6	155	309
$[\text{Ala}_9 - \text{H}]^-$	656.30	62.84	2.54	238.5	1 236.2	167	333
$[\text{Ala}_{10} - \text{H}]^-$	727.33	70.04	2.92	252.8	1 313.0	179	357
$[\text{Ala}_{11} - \text{H}]^-$	798.37	76.98	3.29	266	1 383.8	190	379
$[\text{Ala}_{12} - \text{H}]^-$	869.40	84.13	3.68	278.2	1 449.3	200	399
$[\text{Ala}_{13} - \text{H}]^-$	940.43	92.29	4.11	292.8	1 527.1	213	425
$[1 - \text{H}]^-$	381.10	35.71	1.09	190.5	973.1	116.7	232.3
$[2 - \text{H}]^-$	437.16	44.18	1.54	207.7	1 065.7	133.9	266.7
$[3 - \text{H}]^-$	436.17	47.19	1.70	215.9	1 107.7	140.1	279.0
$[4 - \text{H}]^-$	464.20	52.05	1.96	222.4	1 143.1	146.8	292.4
$[5 - \text{H}]^-$	519.26	65.02	2.66	248.6	1 281.7	167.2	333.2
$[1 + \text{Cl}]^-$	417.08	38.01	1.21	194.3	995.5	122.3	243.5
$[2 + \text{Cl}]^-$	473.14	46.30	1.65	212.5	1 092.8	139.2	277.3
$[3 + \text{Cl}]^-$	472.14	49.88	1.85	218.8	1 125.2	143.2	285.3
$[4 + \text{Cl}]^-$	500.17	48.22	1.76	213.2	1 098.1	138.9	276.8
$[5 + \text{Cl}]^-$	555.24	58.44	2.30	231.9	1 197.6	156.0	311.0

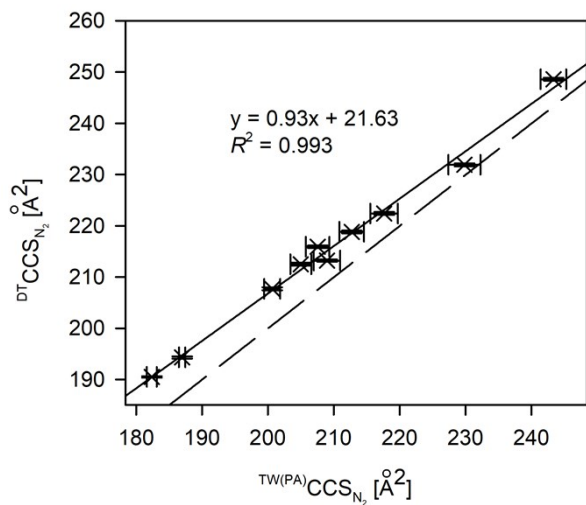


Figure S2.1. Relationship between directly (DTIM-MS) measured $^{DT}CCS_{N_2}$ values and indirectly measured (TWIM-MS) values using polyalanine calibration. Dashed line represents the desired relationship ($y = x$) between the considered values.

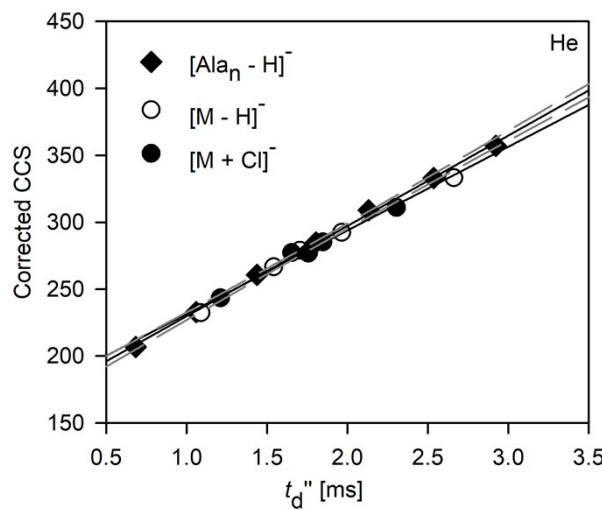


Figure S2.2. Relationship between the calibration plots (He) for deprotonated polyalanine ions ($[Ala_n, n = 4 - 10]$) and macrocyclic ions: $[M - H]^-$ and $[M + Cl]^-$ obtained for N_2 drift gases (recorded at ratios of traveling wave velocity [m/s] to wave height [V]: 350/29). The 95% confidential bands for polyalanine plot is shown.

Table S2.2. ${}^{TW(PA)}CCS$ values [\AA^2] of macrocyclic ions $[\text{M} - \text{H}]^-$ and $[\text{M} + \text{Cl}]^-$ estimated based on the calibration plots (linear or power regression) using polyalanine anions. N_2 was used as a drift gas. CCS values of polyalanine ions for N_2 and He were applied in the calibration procedure to obtain ${}^{TW(PA)}CCS_{\text{N}2}$ and ${}^{TW(PA)}CCS_{\text{He(N}2)}$, respectively. Standard errors, SE (for a 95% level of confidence) of the estimated values and difference between ${}^{TW(PA)}CCS$ values and ${}^{DT}CCS$ (ΔCCS) are reported.

Ion	${}^{TW(PA)}CCS_{\text{N}2}$	SE	ΔCCS	$\Delta CCS \%$	${}^{TW(PA)}CCS_{\text{He(N}2)}$	SE	ΔCCS	$\Delta CCS \%$
[1 - H]⁻	182.4	0.8	-4.3	-2.2	119	1	2	1
[2 - H]⁻	200.6	1.2	-3.4	-1.6	135	1	0	0
[3 - H]⁻	207.5	1.8	-3.9	-1.8	140	1	0	0
[4 - H]⁻	217.6	2.1	-2.1	-1.0	149	2	1	1
[5 - H]⁻	243.3	1.9	-2.1	-0.9	170	1	2	1
[1 + Cl]⁻	187.0	0.5	-3.8	-1.9	123	1	1	0
[2 + Cl]⁻	205.0	1.6	-3.5	-1.7	138	1	-1	0
[3 + Cl]⁻	212.7	1.9	-2.8	-1.3	145	2	1	1
[4 + Cl]⁻	209.0	2.0	-2.0	-0.9	142	2	2	2
[5 + Cl]⁻	229.8	2.4	-0.9	-0.4	160	1	2	1

Table S2.3. Detailed TWIM-experimental values (arrival time values, AT), calibration parameters (corrected drift time, t_d'' , corrected CCS, R^2 for a calibration plot – linear or power regression) and estimated $^{TW(PA)}CCS$ values across various drift tube parameters (WV [m/s] and WH [V]).

a) WV/WH: 350/29

Ion	m/z	Arrival Time (AT)	t_d'' [ms]	Corrected CCS _{N₂}	Corrected CCS _{He(N₂)}
[Ala ₄ - H] ⁻	301.13	28.09	0.68	837.8	207
[Ala ₅ - H] ⁻	372.16	35.15	1.06	921.8	233
[Ala ₆ - H] ⁻	443.20	42.26	1.44	1007.1	261
[Ala ₇ - H] ⁻	514.23	49.13	1.80	1083.9	285
[Ala ₈ - H] ⁻	585.27	55.29	2.13	1156.6	309
[Ala ₉ - H] ⁻	656.30	62.84	2.54	1236.2	333
[Ala ₁₀ - H] ⁻	727.33	70.04	2.92	1313.0	357
[Ala ₁₁ - H] ⁻	798.37	76.98	3.29	1383.8	379
[Ala ₁₂ - H] ⁻	869.40	84.13	3.68	1449.3	399
[Ala ₁₃ - H] ⁻	940.43	92.29	4.11	1527.1	425
				$^{TW(PA)}CCS_{N_2}$ ($R^2 = 0.998$)	$^{TW(PA)}CCS_{He(N_2)}$ ($R^2 = 0.998$)
[1 - H] ⁻	381.10	35.71	1.09	182.9	119
[2 - H] ⁻	437.16	44.18	1.54	199.9	134
[3 - H] ⁻	436.17	47.19	1.70	206.3	139
[4 - H] ⁻	464.20	52.05	1.96	216.1	147
[5 - H] ⁻	519.26	65.02	2.66	242.7	169
[1 + Cl] ⁻	417.08	38.01	1.21	187.1	123
[2 + Cl] ⁻	473.14	46.30	1.65	203.8	137
[3 + Cl] ⁻	472.14	49.88	1.85	211.4	143
[4 + Cl] ⁻	500.17	48.22	1.76	207.5	141
[5 + Cl] ⁻	555.24	58.44	2.30	228.4	158

b) WV/WH:400/29

Ion	<i>m/z</i>	Arrival Time (AT)	<i>t_d</i> " [ms]	Corrected CCS _{N₂}	Corrected CCS _{He(N₂)}
[Ala ₄ - H] ⁻	301.13	34.26	1.11	837.8	207
[Ala ₅ - H] ⁻	372.16	41.76	1.51	921.8	233
[Ala ₆ - H] ⁻	443.20	49.30	1.92	1007.1	261
[Ala ₇ - H] ⁻	514.23	56.96	2.32	1083.9	285
[Ala ₈ - H] ⁻	585.27	63.55	2.68	1156.6	309
[Ala ₉ - H] ⁻	656.30	71.41	3.10	1236.2	333
[Ala ₁₀ - H] ⁻	727.33	79.54	3.53	1313.0	357
[Ala ₁₁ - H] ⁻	798.37	88.01	3.99	1383.8	379
[Ala ₁₂ - H] ⁻	869.40	96.40	4.44	1449.3	399
[Ala ₁₃ - H] ⁻	940.43	105.65	4.93	1527.1	425
				^{TW(PA)} CCS _{N₂} (<i>R</i> ² = 0.996)	^{TW(PA)} CCS _{He(N₂)} (<i>R</i> ² = 0.998)
[1 - H] ⁻	381.11	42.16	1.53	183.1	119
[2 - H] ⁻	437.17	51.33	2.03	199.6	136
[3 - H] ⁻	436.17	54.67	2.21	206.0	142
[4 - H] ⁻	464.21	60.11	2.50	215.8	151
[5 - H] ⁻	519.27	73.86	3.24	241.1	171
[1 + Cl] ⁻	417.08	44.61	1.66	187.1	124
[2 + Cl] ⁻	473.15	53.71	2.15	203.6	140
[3 + Cl] ⁻	472.15	57.67	2.37	211.1	147
[4 + Cl] ⁻	500.18	55.85	2.27	207.2	144
[5 + Cl] ⁻	555.25	66.71	2.85	227.1	161

c) WV/WH: 450/27

Ion	<i>m/z</i>	Arrival Time (AT)	<i>t_d</i> " [ms]	Corrected CCS _{N₂}	Corrected CCS _{He(N₂)}
[Ala ₄ - H] ⁻	301.13	44.55	1.75	837.8	207
[Ala ₅ - H] ⁻	372.17	53.62	2.23	921.8	233
[Ala ₆ - H] ⁻	443.20	62.54	2.71	1007.1	261
[Ala ₇ - H] ⁻	514.24	71.79	3.20	1083.9	285
[Ala ₈ - H] ⁻	585.27	80.21	3.65	1156.6	309
[Ala ₉ - H] ⁻	656.31	90.80	4.22	1236.2	333
[Ala ₁₀ - H] ⁻	727.34	101.24	4.78	1313.0	357
[Ala ₁₁ - H] ⁻	798.38	111.87	5.35	1383.8	379
[Ala ₁₂ - H] ⁻	869.41	122.43	5.92	1449.3	399
[Ala ₁₃ - H] ⁻	940.44	134.18	6.55	1527.1	425
				^{TW(PA)} CCS _{N₂} ($R^2 = 0.999$)	^{TW(PA)} CCS _{He(N₂)} ($R^2 = 1$)
[1 - H] ⁻	381.11	54.13	2.26	182.2	119
[2 - H] ⁻	437.17	65.00	2.84	201.5	135
[3 - H] ⁻	436.18	68.87	3.05	208.2	140
[4 - H] ⁻	464.21	75.74	3.42	219.0	149
[5 - H] ⁻	519.27	94.18	4.41	245.4	171
[1 + Cl] ⁻	417.09	57.14	2.42	187.5	123
[2 + Cl] ⁻	473.15	67.76	2.99	205.8	138
[3 + Cl] ⁻	472.15	72.64	3.25	213.9	145
[4 + Cl] ⁻	500.18	70.18	3.12	209.5	141
[5 + Cl] ⁻	555.25	84.32	3.88	230.9	159

d) WV/WH: 550/29

Ion	<i>m/z</i>	Arrival Time (AT)	<i>t_d</i> " [ms]	Corrected CCS _{N2}	Corrected CCS _{He(N2)}
[Ala ₄ - H] ⁻	301.13	29.35	1.04	837.8	207
[Ala ₅ - H] ⁻	372.17	35.05	1.34	921.8	233
[Ala ₆ - H] ⁻	443.20	40.92	1.65	1007.1	261
[Ala ₇ - H] ⁻	514.24	46.85	1.97	1083.9	285
[Ala ₈ - H] ⁻	585.27	51.82	2.23	1156.6	309
[Ala ₉ - H] ⁻	656.31	57.87	2.55	1236.2	333
[Ala ₁₀ - H] ⁻	727.34	64.08	2.89	1313.0	357
[Ala ₁₁ - H] ⁻	798.38	70.68	3.24	1383.8	379
[Ala ₁₂ - H] ⁻	869.41	77.11	3.58	1449.3	399
[Ala ₁₃ - H] ⁻	940.44	84.13	3.96	1527.1	425
				^{TW(PA)} CCS _{N2} ($R^2 = 0.998$)	^{TW(PA)} CCS _{He(N2)} ($R^2 = 0.999$)
[1 - H] ⁻	381.11	35.27	1.35	181.6	118
[2 - H] ⁻	437.17	42.19	1.72	201.8	135
[3 - H] ⁻	436.18	44.92	1.87	209.5	141
[4 - H] ⁻	464.21	48.90	2.08	219.6	149
[5 - H] ⁻	519.27	59.21	2.63	243.7	170
[1 + Cl] ⁻	417.09	37.06	1.44	186.5	123
[2 + Cl] ⁻	473.15	44.09	1.82	205.1	138
[3 + Cl] ⁻	472.15	47.01	1.98	212.6	144
[4 + Cl] ⁻	500.18	45.91	1.92	209.4	141
[5 + Cl] ⁻	555.26	54.24	2.36	231.0	160

e) WV/WH: 650/39

Ion	<i>m/z</i>	Arrival Time (AT)	<i>t_d</i> " [ms]	Corrected CCS _{N₂}	Corrected CCS _{He(N₂)}
[Ala ₄ - H] ⁻	301.14	35.25	1.43	837.8	207
[Ala ₅ - H] ⁻	372.17	41.87	1.78	921.8	233
[Ala ₆ - H] ⁻	443.21	48.17	2.12	1007.1	261
[Ala ₇ - H] ⁻	514.24	55.00	2.48	1083.9	285
[Ala ₈ - H] ⁻	585.28	61.23	2.82	1156.6	309
[Ala ₉ - H] ⁻	656.31	68.74	3.22	1236.2	333
[Ala ₁₀ - H] ⁻	727.35	76.18	3.62	1313.0	357
[Ala ₁₁ - H] ⁻	798.38	84.00	4.04	1383.8	379
[Ala ₁₂ - H] ⁻	869.42	91.69	4.45	1449.3	399
[Ala ₁₃ - H] ⁻	940.45	100.06	4.90	1527.1	425
				^{TW(PA)} CCS _{N₂} (<i>R</i> ² = 1)	^{TW(PA)} CCS _{He(N₂)} (<i>R</i> ² = 1)
[1 - H] ⁻	381.11	42.19	1.80	182.1	119
[2 - H] ⁻	437.17	49.80	2.21	200.4	134
[3 - H] ⁻	436.18	52.90	2.38	207.8	140
[4 - H] ⁻	464.21	57.42	2.62	217.5	148
[5 - H] ⁻	519.28	70.46	3.32	243.7	170
[1 + Cl] ⁻	417.09	44.11	1.90	186.7	123
[2 + Cl] ⁻	473.15	52.03	2.33	206.6	139
[3 + Cl] ⁻	472.16	55.25	2.50	214.6	145
[4 + Cl] ⁻	500.18	54.03	2.43	211.2	143
[5 + Cl] ⁻	555.25	64.38	2.99	231.7	160

Table S2.4. CCS determination of $[1 + X]^-$ complexes. TWIM-experimental values (AT and t_d'' for reference ions and for measured complexes) for two sets of measurements a) $X^- = \text{AcO}^-$, Br^- , HSO_4^- , SA^- and b) F^- , NO_2^- , NO_3^- , H_2PO_4^- , PhCOO^- , depending on examined various drift tube parameters (WV [m/s] and WH [V]).

Ion	<i>m/z</i>	a)					
		WV/WH = 350/29		WV/WH = 400/29		WV/WH = 450/27	
		<i>AT</i>	t_d'' [ms]	<i>AT</i>	t_d'' [ms]	<i>AT</i>	t_d'' [ms]
$[\text{Ala}_4 - \text{H}]^-$	301.1	28.33	0.69	34.57	1.13	44.77	1.76
$[\text{Ala}_5 - \text{H}]^-$	372.2	35.44	1.07	42.02	1.53	53.77	2.24
$[\text{Ala}_6 - \text{H}]^-$	443.2	42.64	1.46	49.71	1.94	62.97	2.73
$[\text{Ala}_7 - \text{H}]^-$	514.2	49.46	1.82	57.30	2.34	72.18	3.22
$[\text{Ala}_8 - \text{H}]^-$	585.3	55.65	2.15	63.98	2.70	80.71	3.68
$[\text{Ala}_9 - \text{H}]^-$	656.3	63.14	2.55	71.85	3.12	91.31	4.25
$[\text{Ala}_{10} - \text{H}]^-$	727.3	70.38	2.94	79.99	3.56	101.82	4.81
$[\text{Ala}_{11} - \text{H}]^-$	798.4	77.27	3.31	88.46	4.01	112.50	5.39
$[\text{Ala}_{12} - \text{H}]^-$	869.4	84.53	3.70	96.82	4.46	123.11	5.96
$[\text{Ala}_{13} - \text{H}]^-$	940.4	92.64	4.13	106.08	4.96	135.00	6.59
$[\mathbf{1} - \text{H}]^-$	381.1	35.87	1.10	42.34	1.54	54.32	2.27
$[\mathbf{2} - \text{H}]^-$	437.2	44.36	1.55	51.63	2.04	65.27	2.86
$[\mathbf{3} - \text{H}]^-$	436.2	47.46	1.72	54.91	2.22	69.11	3.06
$[\mathbf{4} - \text{H}]^-$	464.2	52.17	1.97	60.34	2.51	76.08	3.44
$[\mathbf{5} - \text{H}]^-$	519.3	65.05	2.66	74.00	3.24	94.30	4.42
$[\mathbf{1} + \text{Cl}]^-$	417.1	38.14	1.22	44.89	1.68	57.32	2.43
$[\mathbf{2} + \text{Cl}]^-$	473.1	46.61	1.67	53.93	2.16	68.01	3.00
$[\mathbf{3} + \text{Cl}]^-$	472.1	50.06	1.86	57.95	2.38	73.04	3.27
$[\mathbf{4} + \text{Cl}]^-$	500.2	48.28	1.76	56.01	2.27	70.39	3.13
$[\mathbf{5} + \text{Cl}]^-$	555.2	58.55	2.31	66.95	2.86	84.59	3.89
$[\mathbf{1} + \text{AcO}]^-$	441.1	42.00	1.42	49.08	1.90	62.37	2.70
$[\mathbf{1} + \text{Br}]^-$	461.0	38.98	1.26	45.64	1.72	57.89	2.46
$[\mathbf{1} + \text{HSO}_4]^-$	479.1	43.67	1.51	50.87	2.00	64.52	2.81
$[\mathbf{1} + \text{SA}]^-$	519.1	51.53	1.93	59.76	2.48	75.42	3.40

b)

Ion	<i>m/z</i>	WV/WH = 350/29		WV/WH = 400/29		WV/WH = 450/27	
		AT	<i>t_d"</i> [ms]	AT	<i>t_d"</i> [ms]	AT	<i>t_d"</i> [ms]
[Ala ₄ - H] ⁻	301.1	28.18	0.69	34.41	1.12	44.69	1.75
[Ala ₅ - H] ⁻	372.2	35.24	1.06	41.90	1.52	53.70	2.23
[Ala ₆ - H] ⁻	443.2	42.37	1.44	49.48	1.93	62.90	2.73
[Ala ₇ - H] ⁻	514.2	49.19	1.81	57.05	2.33	72.05	3.22
[Ala ₈ - H] ⁻	585.3	55.39	2.14	63.74	2.69	80.54	3.67
[Ala ₉ - H] ⁻	656.3	62.92	2.54	71.54	3.10	91.11	4.24
[Ala ₁₀ - H] ⁻	727.3	70.15	2.93	79.69	3.54	101.56	4.80
[Ala ₁₁ - H] ⁻	798.4	77.14	3.30	88.21	4.00	112.28	5.37
[Ala ₁₂ - H] ⁻	869.4	84.34	3.69	96.66	4.45	122.83	5.94
[Ala ₁₃ - H] ⁻	940.4	92.52	4.13	105.90	4.95	134.68	6.58
[1 - H] ⁻	381.1	35.79	1.09	42.23	1.54	54.21	2.26
[2 - H] ⁻	437.2	44.24	1.54	51.47	2.03	65.14	2.85
[3 - H] ⁻	436.2	47.24	1.71	54.72	2.21	68.93	3.05
[4 - H] ⁻	464.2	52.15	1.97	60.31	2.51	76.00	3.43
[5 - H] ⁻	519.3	65.16	2.67	74.14	3.25	94.41	4.42
[1 + Cl] ⁻	417.1	38.05	1.21	44.75	1.67	57.18	2.42
[2 + Cl] ⁻	473.1	46.32	1.65	53.75	2.15	67.82	2.99
[3 + Cl] ⁻	472.1	50.01	1.85	57.84	2.38	72.88	3.26
[4 + Cl] ⁻	500.2	48.21	1.75	55.91	2.27	70.12	3.11
[5 + Cl] ⁻	555.2	58.57	2.31	66.95	2.86	84.45	3.88
[1 + F] ⁻	401.1	37.16	1.16	43.81	1.62	55.70	2.34
[1 + NO ₂] ⁻	428.1	39.29	1.28	46.04	1.74	57.93	2.46
[1 + NO ₃] ⁻	444.1	40.88	1.36	47.68	1.83	59.36	2.54
[1 + H ₂ PO ₄] ⁻	479.1	44.19	1.54	51.37	2.03	64.98	2.84
[1 + PhCOO] ⁻	503.2	50.36	1.87	58.44	2.41	73.77	3.31

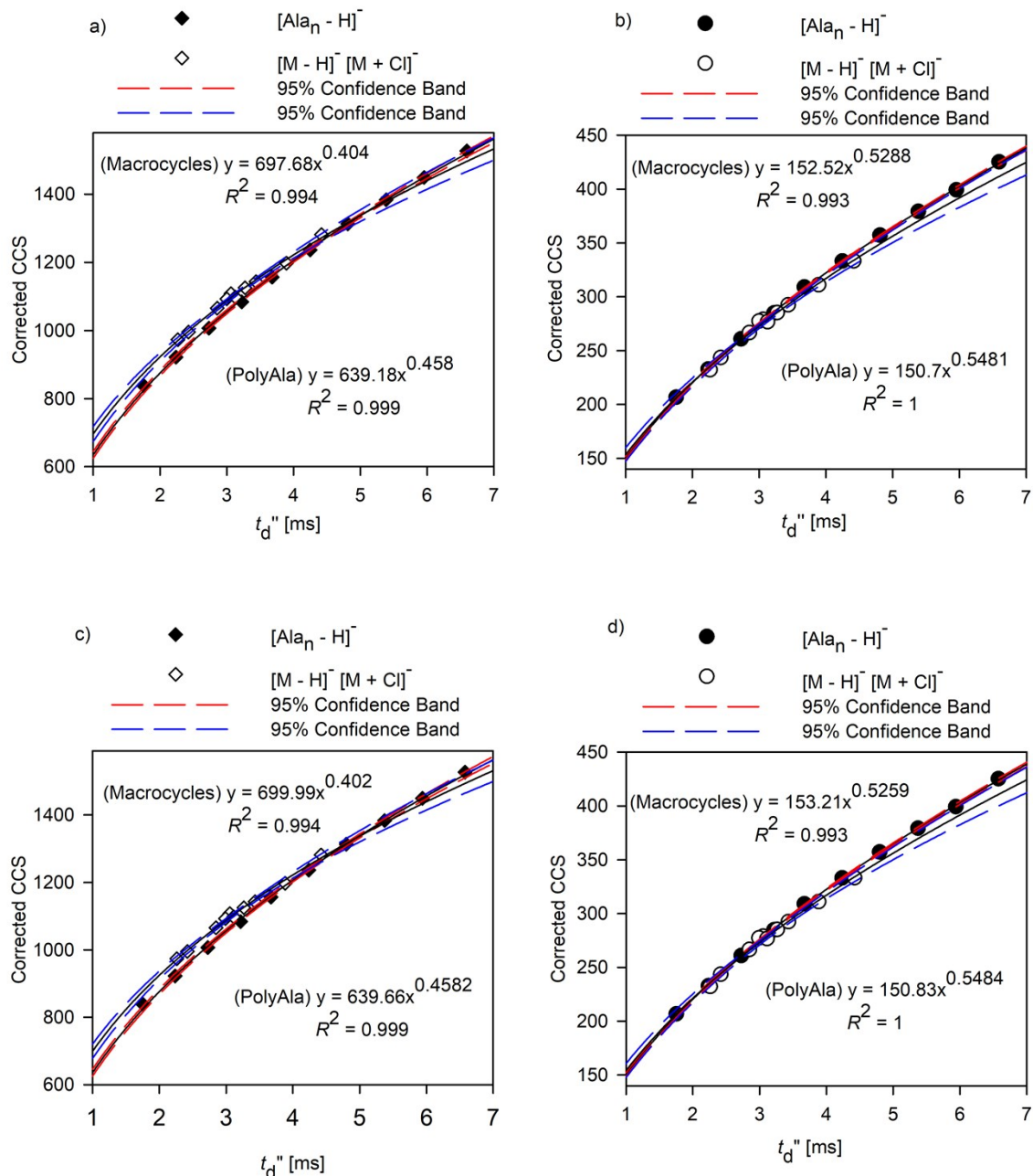


Figure S2.3. CCS determination of **1 + X⁻** complexes. Calibration plots for polyalanine ($[\text{Ala}_n - \text{H}]^-$) and macrocyclic $[\text{M} - \text{H}]^-$ and $[\text{M} + \text{Cl}]^-$ reference ions recorded at WV/WH = 450/27, according to the values reported in Table S2.4. The reference values of CCS based in N₂ (a and c) and He (b and d) were applied in the calibration procedures. The results for two groups of anions are reported.

Table S2.5. ${}^{TW(M)}CCS$ and ${}^{TW(PA)}CCS$ values [\AA^2] of $[1 + X]^-$ complexes estimated based on the calibration plots (linear or power regression) using both polyalanine and macrocycle anions. N_2 was used as a drift gas. Reference CCS values of polyalanine ions and macrocyclic anions (both $[M - H]^-$ and $[M + Cl]^-$ for N_2 and He were applied in the calibration procedure to obtained ${}^{TW}CCS_{N_2}$ and ${}^{TW}CCS_{He(N_2)}$, respectively. Standard errors SE (for a 95% level of confidence) of the estimated values are reported [\AA^2].

Ion	<i>m/z</i>	${}^{TW(M)}CCS_{N_2}$	SE	${}^{TW(PA)}CCS_{N_2}$	SE
$[1 + F]^-$	401.1	193.3	1.7	185.2	1.4
$[1 + Cl]^-$	417.1	194.7	1.3	186.7	0.4
$[1 + Br]^-$	461.0	195.7	1.2	187.8	0.3
$[1 + NO_2]^-$	428.1	197.0	2.1	189.1	1.5
$[1 + NO_3]^-$	444.1	199.6	3.1	191.9	2.3
$[1 + AcO]^-$	441.1	202.7	0.7	195.1	2.4
$[1 + PhCOO]^-$	503.1	219.2	1.6	212.8	4.4
$[1 + SA]^-$	519.1	221.2	1.5	214.8	5.0
$[1 + HSO_4]^-$	479.1	205.5	0.9	198.1	2.9
$[1 + H_2PO_4]^-$	479.1	206.7	0.6	199.5	2.3
		${}^{TW(M)}CCS_{He(N_2)}$	SE	${}^{TW(PA)}CCS_{He(N_2)}$	SE
$[1 + F]^-$		120.2	0.6	121.4	0.5
$[1 + Cl]^-$		121.8	0.2	122.8	0.9
$[1 + Br]^-$		123.2	0.3	124.2	1.1
$[1 + NO_2]^-$		124.0	1.2	125.1	1.0
$[1 + NO_3]^-$		126.7	2.7	127.7	1.5
$[1 + AcO]^-$		129.4	0.1	130.4	2.3
$[1 + PhCOO]^-$		144.4	0.3	145.9	1.8
$[1 + SA]^-$		146.2	0.4	147.6	4.7
$[1 + HSO_4]^-$		132.4	0.4	133.3	2.7
$[1 + H_2PO_4]^-$		133.4	0.8	134.4	1.1

Table S2.6. CCS determination of $[5 + X]^-$ complexes. TWIM-experimental values (AT and t_d'' for reference ions and for measured complexes) for two sets of measurements a) $X = \text{AcO}^-$, Br^- , HSO_4^- , SA^- and b) F^- , NO_2^- , NO_3^- , H_2PO_4^- , PhCOO^- , depending on examined various drift tube parameters (WV [m/s] and WH [V]).

Ion	<i>m/z</i>	a)							
		WV/WH = 350/29		WV/WH = 400/29		WV/WH = 450/27		WV/WH = 550/29	
		AT	t_d'' [ms]						
$[\text{Ala}_4 - \text{H}]^-$	301.1	28.41	0.70	34.56	1.13	44.77	1.76	29.53	1.05
$[\text{Ala}_5 - \text{H}]^-$	372.2	35.13	1.06	41.97	1.52	53.79	2.24	35.17	1.35
$[\text{Ala}_6 - \text{H}]^-$	443.2	42.60	1.46	49.63	1.93	62.69	2.72	41.04	1.66
$[\text{Ala}_7 - \text{H}]^-$	514.2	49.48	1.82	57.28	2.34	71.87	3.21	46.97	1.97
$[\text{Ala}_8 - \text{H}]^-$	585.2	55.68	2.15	63.95	2.70	80.22	3.65	51.96	2.24
$[\text{Ala}_9 - \text{H}]^-$	656.3	63.27	2.56	71.97	3.13	91.47	4.26	58.14	2.57
$[\text{Ala}_{10} - \text{H}]^-$	727.3	70.52	2.95	80.07	3.56	101.83	4.81	64.35	2.90
$[\text{Ala}_{11} - \text{H}]^-$	798.3	77.50	3.32	88.60	4.02	112.56	5.39	70.97	3.25
$[\text{Ala}_{12} - \text{H}]^-$	869.4	84.77	3.71	97.00	4.47	123.36	5.97	77.60	3.61
$[\text{Ala}_{13} - \text{H}]^-$	940.4	92.87	4.14	106.21	4.96	135.18	6.60	84.57	3.98
$[\mathbf{1} - \text{H}]^-$	381.1	35.82	1.09	42.28	1.54	54.25	2.26	35.38	1.36
$[\mathbf{2} - \text{H}]^-$	437.2	44.46	1.56	51.53	2.04	65.12	2.85	42.35	1.73
$[\mathbf{3} - \text{H}]^-$	436.2	47.25	1.71	54.75	2.21	68.91	3.05	44.99	1.87
$[\mathbf{4} - \text{H}]^-$	464.2	52.20	1.97	60.27	2.51	75.83	3.42	49.00	2.09
$[\mathbf{5} - \text{H}]^-$	519.2	65.43	2.68	74.53	3.27	95.18	4.47	59.69	2.66
$[\mathbf{1} + \text{Cl}]^-$	417.1	38.10	1.21	44.84	1.68	57.23	2.42	37.15	1.45
$[\mathbf{2} + \text{Cl}]^-$	473.1	46.36	1.66	53.81	2.16	67.86	2.99	44.32	1.83
$[\mathbf{3} + \text{Cl}]^-$	472.1	50.02	1.85	57.79	2.37	72.63	3.25	47.08	1.98
$[\mathbf{4} + \text{Cl}]^-$	500.2	48.49	1.77	56.03	2.28	70.23	3.12	46.23	1.93
$[\mathbf{5} + \text{Cl}]^-$	555.2	58.66	2.32	67.07	2.87	84.40	3.88	54.50	2.38
$[\mathbf{5} + \text{AcO}]^-$	579.2	63.92	2.60	73.56	3.22	92.68	4.33	59.50	2.65
$[\mathbf{5} + \text{Br}]^-$	599.2	58.03	2.28	65.96	2.81	82.68	3.79	53.57	2.32
$[\mathbf{5} + \text{HSO}_4]^-$	617.2	63.93	2.60	73.72	3.22	92.83	4.33	59.61	2.65
$[\mathbf{5} + \text{SA}]^-$	657.2	72.88	3.08	83.67	3.76	106.62	5.08	66.99	3.05

b)

Ion	<i>m/z</i>	WV/WH = 350/29		WV/WH = 400/29		WV/WH = 450/27		WV/WH = 550/29	
		AT	<i>t_d" [ms]</i>						
[Ala ₄ - H] ⁻	301.1	28.35	0.70	34.45	1.12	44.60	1.75	29.42	1.04
[Ala ₅ - H] ⁻	372.2	35.36	1.07	41.87	1.52	53.62	2.23	35.10	1.34
[Ala ₆ - H] ⁻	443.2	42.43	1.45	49.40	1.92	62.50	2.71	40.96	1.65
[Ala ₇ - H] ⁻	514.2	49.26	1.81	57.05	2.33	71.64	3.19	46.88	1.97
[Ala ₈ - H] ⁻	585.2	55.30	2.13	63.53	2.68	79.43	3.61	51.72	2.23
[Ala ₉ - H] ⁻	656.3	63.56	2.57	72.24	3.14	92.10	4.29	58.48	2.59
[Ala ₁₀ - H] ⁻	727.3	70.55	2.95	80.13	3.56	102.19	4.83	64.52	2.91
[Ala ₁₁ - H] ⁻	798.3	77.44	3.32	88.54	4.02	112.76	5.40	71.02	3.26
[Ala ₁₂ - H] ⁻	869.4	84.73	3.71	97.00	4.47	123.49	5.98	77.62	3.61
[Ala ₁₃ - H] ⁻	940.4	92.75	4.14	106.15	4.96	135.12	6.60	84.56	3.98
[1 - H] ⁻	381.1	35.72	1.09	42.18	1.54	54.10	2.26	35.29	1.35
[2 - H] ⁻	437.2	44.38	1.55	51.40	2.03	65.02	2.84	42.39	1.73
[3 - H] ⁻	436.2	47.12	1.70	54.60	2.20	68.68	3.04	44.90	1.87
[4 - H] ⁻	464.2	54.11	2.08	60.12	2.50	75.69	3.42	48.94	2.08
[5 - H] ⁻	519.2	65.58	2.69	74.55	3.27	95.27	4.47	59.70	2.66
[1 + Cl] ⁻	417.1	37.99	1.21	44.71	1.67	57.07	2.41	37.07	1.44
[2 + Cl] ⁻	473.1	46.27	1.65	54.39	2.19	67.66	2.98	44.20	1.83
[3 + Cl] ⁻	472.1	49.81	1.84	57.51	2.36	72.32	3.23	46.95	1.98
[4 + Cl] ⁻	500.2	48.22	1.76	55.72	2.26	69.99	3.11	46.07	1.93
[5 + Cl] ⁻	555.2	58.58	2.31	66.82	2.85	84.08	3.86	54.35	2.37
[5 + F] ⁻	539.3	69.83	2.92	79.31	3.53	101.20	4.79	63.51	2.87
[5 + NO ₂] ⁻	566.3	59.23	2.35	67.29	2.88	84.71	3.90	54.86	2.40
[5 + NO ₃] ⁻	582.3	61.57	2.47	70.55	3.06	88.26	4.09	57.51	2.54
[5 + H ₂ PO ₄] ⁻	617.2	65.29	2.67	74.12	3.25	93.26	4.36	59.77	2.66
[5 + PhCOO] ⁻	641.3	72.99	3.08	83.01	3.72	105.88	5.04	66.59	3.03

Table S2.7. ${}^{TW(M)}CCS$ and ${}^{TW(PA)}CCS$ values [\AA^2] of $[5 + X]^-$ complexes estimated based on the calibration plots using both polyalanine and macrocycle anions. N₂ was used as a drift gas. Reference CCS values of polyalanine ions and macrocyclic anions (both $[M - H]^-$ and $[M + Cl]^-$ for N₂ and He were applied in the calibration procedure to obtained ${}^{TW}CCS_{N_2}$ and ${}^{TW}CCS_{He(N_2)}$, respectively. Standard errors SE (for a 95% level of confidence) of the estimated values are reported [\AA^2].

Ion	<i>m/z</i>	${}^{TW(M)}CCS_{N_2}$	SE	${}^{TW(PA)}CCS_{N_2}$	SE
$[5 + F]^-$	539.3	255.8	1.7	252.0	2.3
$[5 + Cl]^-$	555.2	234.2	2.2	228.8	3.8
$[5 + Br]^-$	599.2	231.6	1.0	226.7	3.0
$[5 + NO_2]^-$	566.3	234.6	0.9	230.0	3.4
$[5 + NO_3]^-$	582.3	239.8	2.3	235.4	3.7
$[5 + AcO]^-$	579.2	244.9	1.8	240.6	3.4
$[5 + PhCOO]^-$	641.3	260.9	3.0	257.4	1.7
$[5 + SA]^-$	657.2	261.6	3.1	257.9	2.1
$[5 + HSO_4]^-$	617.2	244.7	1.9	240.4	3.5
$[5 + H_2PO_4]^-$	617.2	245.7	1.7	241.6	2.4
		${}^{TW(M)}CCS_{He(N_2)}$	SE	${}^{TW(PA)}CCS_{He(N_2)}$	SE
$[5 + F]^-$		173.0	2.8	177.7	1.1
$[5 + Cl]^-$		156.4	1.3	158.9	2.8
$[5 + Br]^-$		155.2	0.7	157.6	1.8
$[5 + NO_2]^-$		157.3	0.7	160.0	1.8
$[5 + NO_3]^-$		161.4	1.7	164.5	2.6
$[5 + AcO]^-$		165.3	1.5	168.8	2.4
$[5 + PhCOO]^-$		177.3	3.5	182.6	0.8
$[5 + SA]^-$		177.9	3.4	183.1	1.6
$[5 + HSO_4]^-$		165.3	1.7	168.8	2.6
$[5 + H_2PO_4]^-$		166.0	1.2	169.8	1.3

Section S3. Theoretical Computations

S3.1. General Information

Initial optimization was carried out using low cost Grimme's functional including dispersion correction B97D and 6-31G(d') basis set. The conformational minima were selected based on the B97D energies within an energy window of 50 kJ mol⁻¹. Further reoptimization using tight optimization criterion and thermal analysis (1 atm, 298.15 K) were performed using PBE1PBE (PBE0)⁴ hybrid functional and 6-311++G**basis set supplemented with GD3BJ empirical dispersion correction. A quasi-rigid rotor-harmonic oscillator approximation (RRHO) was used to account for low-frequency vibration modes ($\nu < 100 \text{ cm}^{-1}$) and to obtain a correct entropy values using GoodVibes program.⁵ The energies of the complexes were additionally corrected by basis set superposition errors. Detailed report from theoretical studies and geometry specification files are available:

https://www.dropbox.com/s/vbwkvlot3l7mi6r/Calculations_Report.zip?dl=0

It contains: Excel file "Calculations_Report" – B3LYP-D3/6-311++G(d,p) thermochemical properties of the conformers (population above 0.2% according to Boltzmann distribution): E_0 , - electronic energy, $E_0(\text{CP})$ – additionally corrected by basis set superposition errors, ZPV (zero-point vibrational energy), $H_{298 \text{ K}}$ (enthalpy at 298 K), TS (temperature (298 K) x enthalpy), $G_{298\text{K}}(\text{CP})$ – Gibbs free energy at 298 K additionally corrected by basis set superposition errors, population at 298 K, and detailed values of $\text{CCS}_{\text{He}/\text{N}_2}$ (computed with MobCal-MPI, accompanied by standard deviation values) for each conformer. Five folders "Macrocycle 1-5" – containing the xyz coordinates for each conformer reported in Calculations_Report".

S3.2. CCS values prediction

CCS values of ions under studies were computed using MobCal-MPI (v 1.2, installed before March 10) and IMoS mobility software. MobCal-MPI software was recently released for accurate and efficient CCS computations. It is based on the original MobCal software,⁶ but it offers parallelized calculations of ion CCS values in ion-nitrogen van der Waals (vdW) potentially tuned environment. In comparison to the less accurate computational approaches that utilized Lennard-Jones (LJ) potential⁷ to describe the intermolecular interactions between gas molecules and ions, MobCal-MPI utilizes the calibrated vdW parameters of various atom elements (C, H, O, N, F, P, S, Cl, Br, and I). The vdW parameters are complemented by ion-induced dipole and ion-quadrupole potentials, which use atomic partial charges (generated according to the Merz–Singh–Kollman (MK) partition scheme). These additional potentials that are included in the overall MobCal-MPI intermolecular potential model are relevant especially for polarizable gases such as molecular nitrogen, which inherently possess dipole and quadrupole moments. The standard, originally implemented in MobCal-MPI parameters were used. In the case of IMoS the following parameters were applied in the computations:

Gas:	He	N2
Method:	TMLJ (4-6-12 potential)	TMLJ (4-6-12 potential) with quadrupole potential
Temperature:		300 K
Pressure:		526 Pa
Gas molecules per orientation:		1000000
LJ parameters: $\text{eps}(\text{J} \cdot 10^{21})/\sigma(\text{A})$:		
H	0.0989235/2.261	0.2518291316/1.8986165794
C	0.21252132/3.0126	0.5725617712/3.2254869663
O	0.1717344/2.4344	0.4327052508/3.0749947111
N	0.2361348/3.3473	0.5270966235/3.5719061739
F	0.1717344/2.4344	0.3950040443/3.0146504054
Other	0.214668/3.043	0.4167763200/3.5

Table S3.1 Differences between theoretically predicted and experimental CCS values of $[M - H]^-$ and $[M + Cl]^-$. Theoretical CCS values were computed for PBE0 optimized structures using IMOS and MobCal-MPI programs.

Ion/Complex	IMOS (ESP atomic charges)			MobCal-MPI (ESP atomic charges)			IMOS (Mulliken atomic charges)		
	TM CCS(IMOS)	Δ CCS	Δ CCS, %	TM CCS(MobCal-MPI)	Δ CCS	Δ CCS, %	TM CCS(IMOS)	Δ CCS	Δ CCS, %
He									
$[1 - H]^-$	114.6	-2.1	-1.8	115.0	-1.7	-1.5	115.5	-1.2	-1.0
$[2 - H]^-$	131.9	-2.0	-1.5	132.3	-1.6	-1.2	134.1	0.2	0.1
$[3 - H]^-$	135.7	-4.4	-3.1	135.3	-4.8	-3.4	136.9	-3.2	-2.3
$[4 - H]^-$	143.7	-3.1	-2.1	143.4	-3.4	-2.3	144.7	-2.1	-1.4
$[5 - H]^-$	161.0	-6.2	-3.7	160.9	-6.3	-3.8	165.9	-1.3	-0.8
$[5 - H]^{-*}$	164.9	-2.3	-1.4	165.2	-2.0	-1.2			
$[1 + Cl]^-$	119.0	-3.3	-2.7	119.9	-2.4	-2.0	119.7	-2.6	-2.1
$[2 + Cl]^-$	136.9	-2.3	-1.7	137.0	-2.2	-1.6	138.6	-0.6	-0.4
$[3 + Cl]^-$	139.8	-3.4	-2.4	140.9	-2.3	-1.6	140.5	-2.7	-1.9
$[4 + Cl]^-$	134.0	-4.9	-3.5	132.6	-6.3	-4.5	135.1	-3.8	-2.8
$[5 + Cl]^-$	150.3	-5.7	-3.7	148.8	-7.2	-4.6	151.5	-4.5	-2.9
N_2									
$[1 - H]^-$	190.1	-0.4	-0.2	193.0	2.5	1.3	193.1	2.6	1.4
$[2 - H]^-$	207.8	0.1	0.0	210.3	2.6	1.3	220.3	12.6	6.1
$[3 - H]^-$	211.7	-4.2	-1.9	213.2	-2.7	-1.3	218.2	2.3	1.1
$[4 - H]^-$	220.3	-2.1	-0.9	221.9	-0.5	-0.2	226.6	4.2	1.9
$[5 - H]^-$	239.6	-9.0	-3.6	238.3	-10.3	-4.1			
$[5 - H]^{-*}$	244.0	-4.6	-1.9	242.8	-5.8	-2.3	250.8	2.2	0.9
$[1 + Cl]^-$	202.3	8.0	4.1	199.3	5.0	2.6	202.4	8.1	4.2
$[2 + Cl]^-$	216.5	4.0	1.9	217.5	5.0	2.4	225.3	12.8	6.0
$[3 + Cl]^-$	224.2	5.4	2.5	218.9	0.1	0.0	229.2	10.4	4.8
$[4 + Cl]^-$	212.1	-1.1	-0.5	209.7	-3.5	-1.6	218.2	5.0	2.4
$[5 + Cl]^-$	227.4	-4.5	-1.9	225.6	-6.3	-2.7	234.3	2.4	1.0

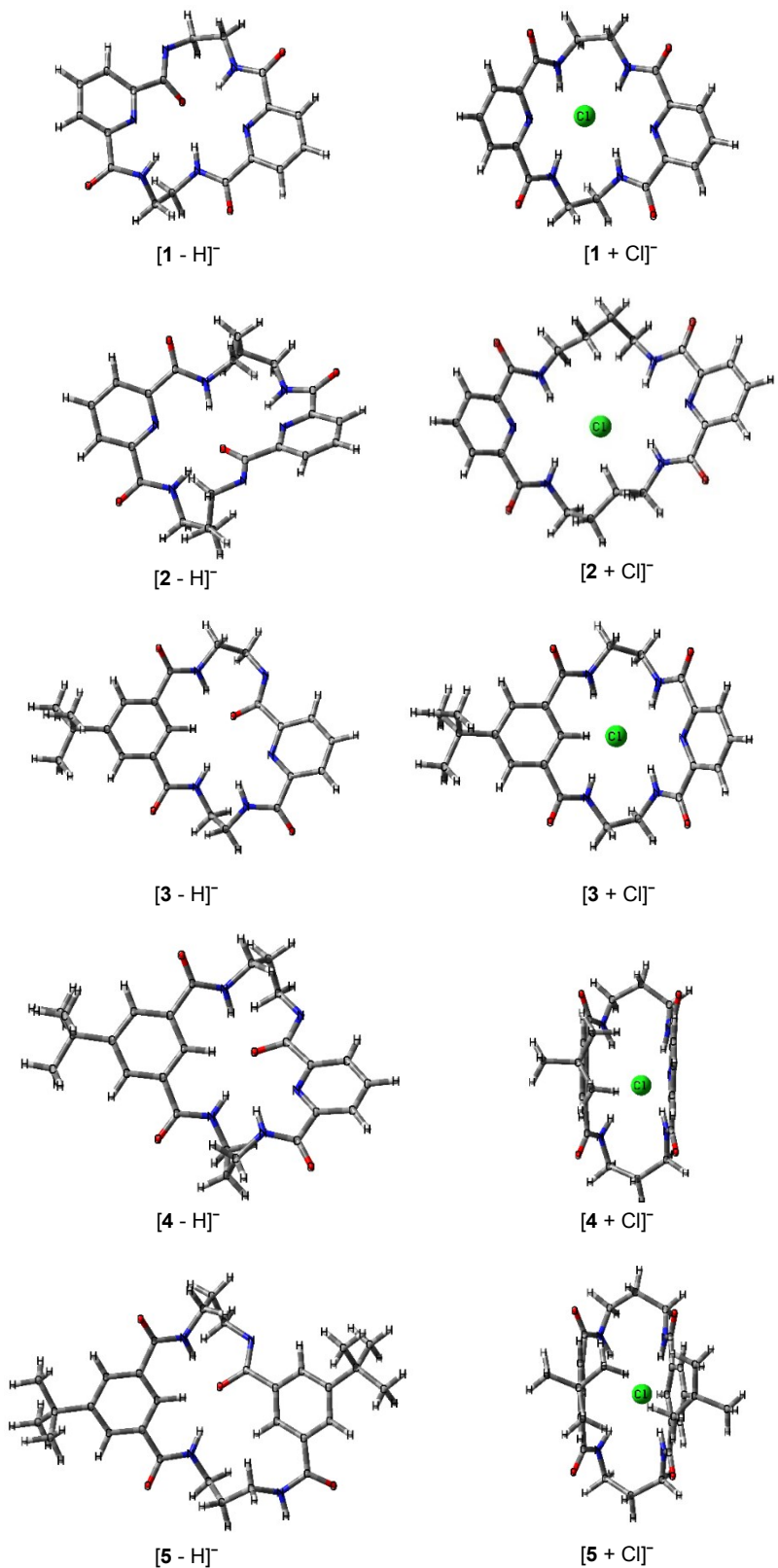


Figure S3.1. Structures of the lowest-energy conformers of deprotonated and chloride adducts of macrocycles **1-5** (view on a mean plane of macrocyclic ring).

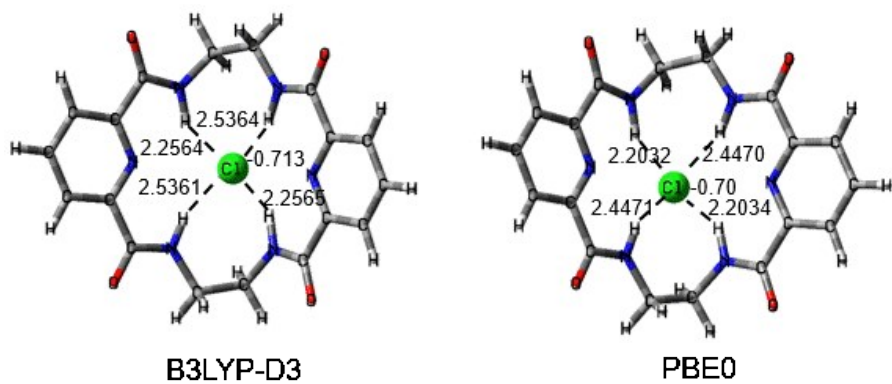


Figure S3.2. Differences in bond lengths and partial charges on Cl^- of the most stable structures $[1 + \text{Cl}]^-$ calculated with B3LYP and PBE0 methods.

Table S3.2. Theoretically predicted ${}^{\text{TM}}\text{CCS}$ values [\AA^2] of $[\mathbf{1} + \text{X}]^-$ using MobCal-MPI and IMOS mobility programs along with the standard deviations (SD) of the computed values. ΔCCS [\AA^2] expresses the differences between theoretically predicted and experimental (${}^{\text{TW(M)}}\text{CCS}_{\text{N}_2}$ and ${}^{\text{TW(M)}}\text{CCS}_{\text{He(N}_2)}$) values.

Complex	MobCal-MPI(B3LYP)				MobCal-MPI(PBEO)			
	CCS	SD	ΔCCS	$\Delta\text{CCS}\%$	CCS	SD	ΔCCS	$\Delta\text{CCS}\%$
N_2								
$[\mathbf{1} + \text{F}]^-$	196.5	2.2	3.2	1.7	194.7	1.6	1.4	0.7
$[\mathbf{1} + \text{Cl}]^-$	200.4	1.0	5.7	2.9	198.4	1.3	3.7	1.9
$[\mathbf{1} + \text{Br}]^-$	201.0	1.6	5.3	2.7	199.9	2.4	4.2	2.2
$[\mathbf{1} + \text{NO}_2]^-$	201.3	1.6	4.4	2.2	200.6	1.4	3.6	1.8
$[\mathbf{1} + \text{NO}_3]^-$	203.7	2.0	4.1	2.0	201.7	1.8	2.1	1.0
$[\mathbf{1} + \text{AcO}]^-$	208.7	2.1	6.0	3.0	207.1	1.6	4.4	2.2
$[\mathbf{1} + \text{PhCOO}]^-$	229.4	1.4	10.2	4.7	227.3	1.5	8.1	3.7
$[\mathbf{1} + \text{SA}]^-$	231.6	2.6	10.4	4.7	229.7	1.6	8.5	3.8
$[\mathbf{1} + \text{HSO}_4]^-$	207.7	2.0	2.2	1.1	205.1	1.5	-0.4	-0.2
$[\mathbf{1} + \text{H}_2\text{PO}_4]^-$	213.2	1.6	6.5	3.1	211.2	1.8	4.5	2.2
He								
$[\mathbf{1} + \text{F}]^-$	119.2	1.3	-1.0	-0.8	117.9	1.1	-2.3	-1.9
$[\mathbf{1} + \text{Cl}]^-$	120.5	1.1	-1.3	-1.1	119.9	1.1	-1.9	-1.5
$[\mathbf{1} + \text{Br}]^-$	121.1	1.1	-2.1	-1.7	121.5	1.0	-1.7	-1.4
$[\mathbf{1} + \text{NO}_2]^-$	123.7	1.7	-0.4	-0.3	123.0	1.5	-1.0	-0.8
$[\mathbf{1} + \text{NO}_3]^-$	125.7	1.4	-1.0	-0.8	124.7	1.1	-2.0	-1.6
$[\mathbf{1} + \text{AcO}]^-$	127.3	1.1	-2.1	-1.6	126.8	1.4	-2.6	-2.0
$[\mathbf{1} + \text{PhCOO}]^-$	144.3	1.2	-0.1	-0.1	141.7	1.6	-2.7	-1.9
$[\mathbf{1} + \text{SA}]^-$	145.9	1.5	-0.3	-0.2	145.2	1.5	-1.0	-0.7
$[\mathbf{1} + \text{HSO}_4]^-$	127.0	1.1	-5.3	-4.0	126.2	1.5	-6.2	-4.7
$[\mathbf{1} + \text{H}_2\text{PO}_4]^-$	129.6	1.2	-3.8	-2.8	128.1	1.3	-5.3	-4.0

Table S3.3. Theoretically predicted CCS values [\AA^2] in N_2 and He of polyatomic anions using MobCal-MPI(B3LYP).

Ion	N_2		He	
	CCS	SD	CCS	SD
NO_2^-	107.6	1.4	27.5	0.5
NO_3^-	106.2	0.7	30.4	0.3
AcO^-	115.0	1.2	35.9	0.5
PhCO_2^-	133.6	1.3	54.3	0.6
SA^-	129.1	1.2	55.4	0.5
HSO_4^-	110.9	0.8	36.6	0.2
H_2PO_4^-	119.6	1.4	37.8	0.5

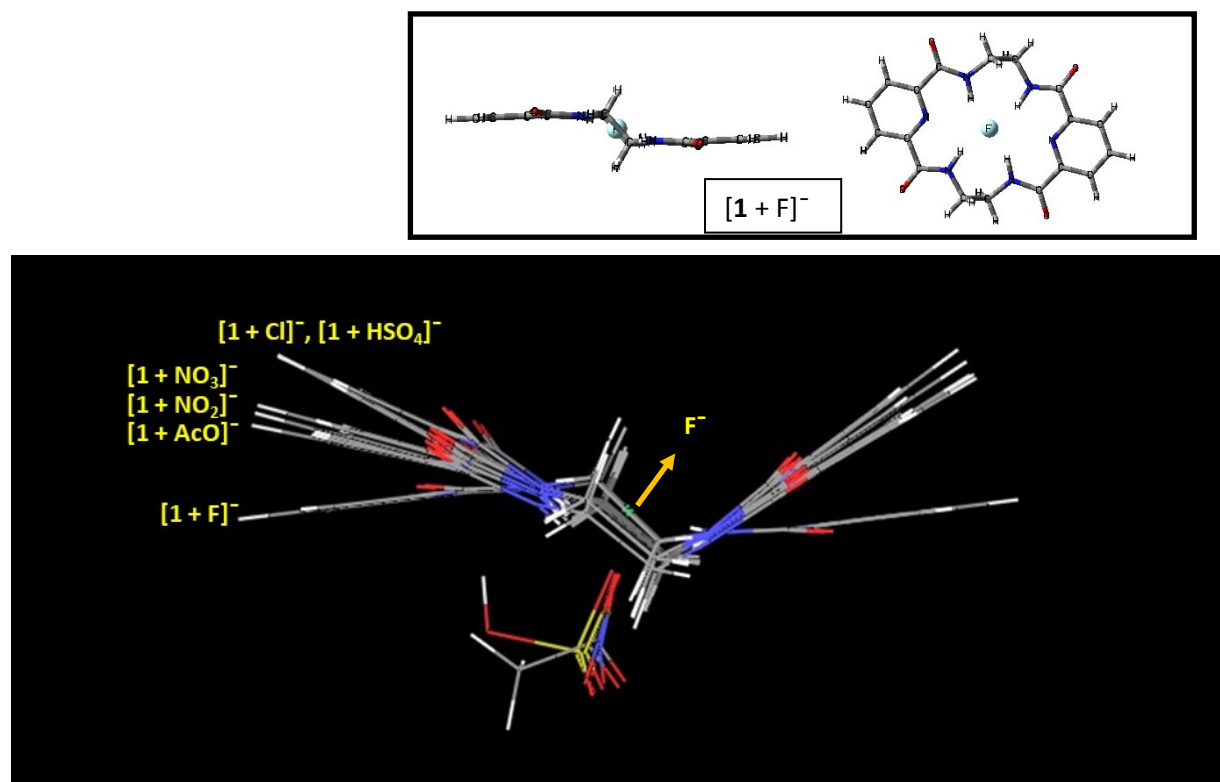


Figure S3.3. Overlapped structures of selected $[1 + X]^-$ complexes represented by parallel conformations. In the figure's inset side and top views of the structure of $[1 + \text{F}]^-$ are presented.

Table S3.4. Theoretically predicted CCS values [\AA^2] of [5 + X]⁻ using MobCal-MPI along with the standard deviations (SD) of the computed values. ΔCCS [\AA^2] expresses the differences between theoretically predicted and experimental (${}^{\text{TW(M)}}\text{CCS}_{\text{N}_2}$ and ${}^{\text{TW(M)}}\text{CCS}_{\text{He(N}_2)}$) values.

Ion	MobCal-MPI(B3LYP)			
	CCS	SD	ΔCCS	$\Delta\text{CCS}\%$
N ₂				
[5 + F] ⁻	245.8	2.5	-9.9	-3.9
[5 + F] ^{-*}	249.9	2.4	-5.8	-2.3
[5 + Cl] ⁻	227.3	2.5	-6.9	-2.9
[5 + Br] ⁻	227.7	2.0	-3.9	-1.7
[5 + NO ₂] ⁻	228.3	2.4	-6.3	-2.7
[5 + NO ₃] ⁻	230.1	2.1	-9.7	-4.0
[5 + AcO] ⁻	234.7	2.1	-10.2	-4.2
[5 + PhCOO] ⁻	254.7	2.3	-6.2	-2.4
[5 + SA] ⁻	256.4	3.1	-5.2	-2.0
[5 + HSO ₄] ⁻	235.3	2.1	-9.4	-3.8
[5 + H ₂ PO ₄] ⁻	237.3	2.2	-8.4	-3.4
He				
[5 + F] ⁻	165.5	1.6	-7.5	-4.3
[5 + F] ^{-*}	168.6	1.5	-4.4	-2.5
[5 + Cl] ⁻	149.9	1.4	-6.5	-4.2
[5 + Br] ⁻	150.0	1.6	-5.2	-3.3
[5 + NO ₂] ⁻	150.9	1.4	-6.4	-4.1
[5 + NO ₃] ⁻	152.8	1.5	-8.6	-5.3
[5 + AcO] ⁻	159.4	1.2	-5.9	-3.6
[5 + PhCOO] ⁻	172.0	1.7	-5.3	-3.0
[5 + SA] ⁻	174.0	1.7	-3.9	-2.2
[5 + HSO ₄] ⁻	156.0	1.5	-9.3	-5.6
[5 + H ₂ PO ₄] ⁻	157.0	1.8	-9.0	-5.4

* Theoretical calculations indicate two distinguished conformations of [5 + F]⁻: open, elongated near planar structure with about $\text{CCS}_{\text{N}_2} = 249.9 \text{ \AA}^2$ and 9 kJmol⁻¹ energetically higher U-shape folded form with $\text{CC}_{\text{N}_2} = 226 \text{ \AA}^2$. The comparison between theoretically predicted and experimental CCS values suggest on the population of the planar conformation in the gas phase, not mixed conformational distribution as predicted from Boltzmann weighted average.

References

1. Stow, S. M.; Causon, T. J.; Zheng, X.; Kurulugama, R. T.; Mairinger, T.; May, J. C.; Rennie, E. E.; Baker, E. S.; Smith, R. D.; McLean, J. A.; Hann, S. Fjeldsted, J. C., An Interlaboratory Evaluation of Drift Tube Ion Mobility-Mass Spectrometry Collision Cross Section Measurements. *Anal. Chem.* **2017**, *89*, 9048-9055.
2. Marchand, A.; Livet, S.; Rosu, F. Gabelica, V., Drift Tube Ion Mobility: How to Reconstruct Collision Cross Section Distributions from Arrival Time Distributions? *Anal. Chem.* **2017**, *89*, 12674-12681.
3. Gabelica, V.; Shvartsburg, A. A.; Afonso, C.; Barran, P.; Benesch, J. L. P.; Bleiholder, C.; Bowers, M. T.; Bilbao, A.; Bush, M. F.; Campbell, J. L.; Campuzano, I. D. G.; Causon, T.; Clowers, B. H.; Creaser, C. S.; De Pauw, E.; Far, J.; Fernandez-Lima, F.; Fjeldsted, J. C.; Giles, K.; Groessl, M.; Hogan Jr, C. J.; Hann, S.; Kim, H. I.; Kurulugama, R. T.; May, J. C.; McLean, J. A.; Pagel, K.; Richardson, K.; Ridgeway, M. E.; Rosu, F.; Sobott, F.; Thalassinos, K.; Valentine, S. J. Wyttenbach, T., Recommendations for reporting ion mobility Mass Spectrometry measurements. *Mass Spectrom. Rev.* **2019**, *38*, 291-320.
4. Adamo, C. Barone, V., Toward reliable density functional methods without adjustable parameters: The PBE0 model. *J. Chem. Phys.* **1999**, *110*, 6158-6170.
5. Luchini, G.; Alegre-Requena, J.; Funes-Ardoiz, I. Paton, R., GoodVibes: automated thermochemistry for heterogeneous computational chemistry data [version 1; peer review: 2 approved with reservations]. *F1000Research* **2020**, *9*.
6. Mesleh, M. F.; Hunter, J. M.; Shvartsburg, A. A.; Schatz, G. C. Jarrold, M. F., Structural Information from Ion Mobility Measurements: Effects of the Long-Range Potential. *J. Phys. Chem.* **1996**, *100*, 16082-16086.
7. Lee, J. W.; Davidson, K. L.; Bush, M. F. Kim, H. I., Collision cross sections and ion structures: development of a general calculation method via high-quality ion mobility measurements and theoretical modeling. *Analyst* **2017**, *142*, 4289-4298.
8. Thalassinos, K.; Grabenauer, M.; Slade, S. E.; Hilton, G. R.; Bowers, M. T. Scrivens, J. H., Characterization of Phosphorylated Peptides Using Traveling Wave-Based and Drift Cell Ion Mobility Mass Spectrometry. *Anal. Chem.* **2009**, *81*, 248-254.